Large cryogenic magnetocaloric effect of $DyCo_2$ nanoparticles without encapsulation

S. Ma,[1,2,a)] W. B. Cui,[1] D. Li,[1] N. K. Sun,[1] D. Y. Geng,[1] X. Jiang,[2] and Z. D. Zhang[1]
[1]*Shenyang National Laboratory for Material Science, Institute of Metal Research, and International Centre for Material Physics, Chinese Academy of Sciences, 72 Wenhua Road, Shenyang 110016, People's Republic of China*
[2]*Institute of Materials Engineering, University of Siegen, Paul-Bonatz-Str. 9-11, 57076 Siegen, Germany*

(Received 28 March 2008; accepted 12 April 2008; published online 1 May 2008)

The structure and formation of nanoparticles without encapsulation of the intermetallic compound $DyCo_2$ were investigated by using x-ray diffraction and high-resolution transmission electron microscopy. The $DyCo_2$ nanoparticles are stable in air without any shell protection. A large magnetic-entropy change of 13.2 J kg^{-1} K^{-1} was found at 7.5 K in an applied-field change from 1 to 7 T, which is ascribed to the large magnetic moment density and the weak interaction energy in the nanoparticles. Such oxidation-resistant rare-earth transition-metal compound nanoparticles with large cryogenic magnetocaloric effect are useful for refrigeration applications at low temperatures. © *2008 American Institute of Physics*. [DOI: 10.1063/1.2919079]

With increasing demands on environmental protection, the conventional refrigeration technologies, which are based on the gas-compression/expansion mechanism, are being gradually replaced by the environment-friendly magnetocaloric techniques. Recently, giant magnetocaloric effects (MCE) have been observed near room temperature at first- or second-order phase transitions.[1–4] At lower temperatures ($T < 20$ K), however, magnetic refrigeration can seldom be realized by employing these types of MCE because these phase transitions usually occur at higher temperatures. As a result, researchers have tried to find large MCE in paramagnetic or superparamagnetic systems.[5–7] However, only little attention has been paid to the possibly large MCE in nanoparticles of magnetic intermetallic compounds composed of rare-earth and transition metals, where the rare-earth atoms have a large magnetic moment. The reason is that rare-earth atoms very easily oxidize in air and the rare-earth transition-metal compounds do not form at nanoscale without shell protection. Although a large magnetic-entropy change ($-\Delta S_M$ representing the magnitude of the MCE) of 18.7 J kg^{-1} K^{-1} has been obtained in the case of $GdAl_2/Al_2O_3$ nanocapsules at 7.5 K in a magnetic-field change (ΔB) of 6 T, the Al_2O_3 shell with low thermal conductivity may decrease their application potential in a refrigeration process.[8]

In this letter, we report on the synthesis of a type of nanoparticles of the intermetallic compound $DyCo_2$ by a modified arc-discharge technique. The $DyCo_2$ nanoparticles have a large $-\Delta S_M$ value of 13.2 J kg^{-1} K^{-1} at 7.5 K at $\Delta B = 6$ T. This work may stimulate the preparation and investigation of other oxidation-resistant nanoparticles with large cryogenic MCE of rare-earth transition-metal compounds.

The $DyCo_2$ nanoparticles were prepared by a modified arc-discharge process similar to the one used in our previous work.[9] A $Dy_{30}Co_{70}$ alloy ingot was used as the anode. When the base vacuum of the arc-discharge chamber reached 7.3×10^{-3} Pa, Ar and H_2 were introduced into the chamber with partial pressures of 2.0×10^4 and 3.0×10^3 Pa, respectively. Then, the arc was started and the discharge current was maintained at 20 A for 5 h. After passivation with fresh Ar gas for 48 h, the product in the form of powder was collected. The phase composition and the microstructure analyses were performed by using powder x-ray diffraction (XRD) with Cu $K\alpha$ and high-resolution transmission electron microscopy (HRTEM) employing 200 kV. The magnetic measurements were carried out in a superconducting quantum interference device magnetometer.

The XRD pattern shown in Fig. 1 reveals that the particles are composed of $DyCo_2$ and Dy_2O_3. The formation mechanism of these two kinds of particles can be explained on the basis of the evaporation of metal atoms and the bumping principle.[8] With a lower boiling point of 2835 K compared to that of Co (3201 K), Dy atoms evaporated more easily into the chamber from the melting pool of the anode alloy. Therefore, the anode composition of Dy:Co=30:70 assures an appropriate Dy/Co ratio in the chamber to form the $DyCo_2$ compound. However, due to the lower boiling point of Dy, there still exists some surplus of evaporated Dy atoms in the chamber, which form Dy particles. Subsequently, the Dy particles are oxidized in the air atmosphere. With other atomic Dy/Co ratios as anode composition, only fcc Co or Dy_2O_3 can be formed. Thus, an appropriate atomic

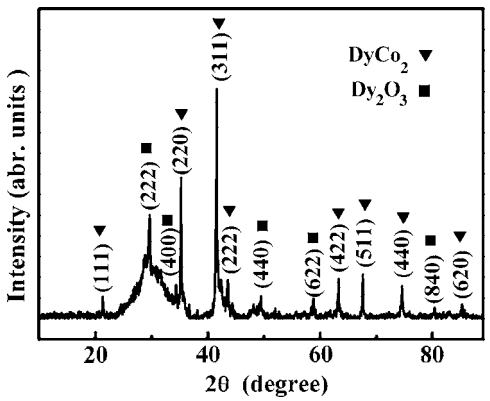

FIG. 1. XRD pattern of the product prepared by arc-discharging $Dy_{30}Co_{70}$ alloy.

a)Electronic mail: song.ma@uni-siegen.de.

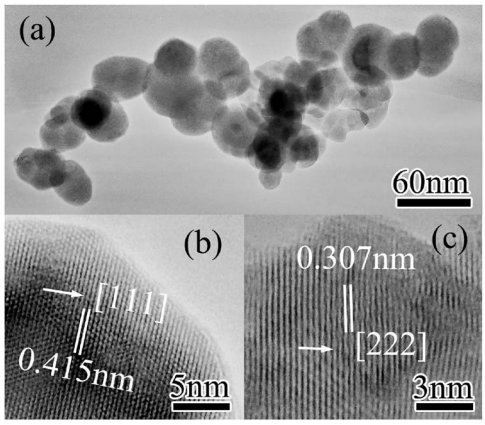

FIG. 2. TEM and HRTEM images of $DyCo_2$ and Dy_2O_3 nanoparticles showing (a) their morphology and size distribution, (b) the lattice fringes of a $DyCo_2$ nanoparticle, and (c) the lattice fringes of a Dy_2O_3 nanoparticle.

ratio of the anode is the most important factor to prepare nanoparticles of the compound $DyCo_2$.

The TEM image [Fig. 2(a)] shows that the morphology of the $DyCo_2$ nanoparticles has an irregular spherical shape and that the distribution of particle diameter is in a range of 15–50 nm. The HRTEM lattice images in Figs. 2(b) and 2(c) show fringe spacings of 0.415 and 0.307 nm that correspond to the characteristic distances of {111} $DyCo_2$ and {222} Dy_2O_3, respectively. It is interesting to note that in Fig. 2(b), no oxide shell can be observed at the surface of the $DyCo_2$ nanoparticle. It shows that the $DyCo_2$ nanoparticles are stable in air without any shell protection. Similar oxidation-resistant behavior may also be expected for other rare-earth containing nanoparticles (for instance, Co- or Ni-based compounds).

The isothermal magnetization curves were measured in a zero-field-cooled (ZFC) process in applied fields up to 7 T. The temperature was varied from 5 to 90 K with steps of 5 K [Fig. 3(a)]. At 5 K and 7 T, the magnetization of $DyCo_2$ is 119 A m^2 kg^{-1}, which almost equals to the corresponding value (123.81 A m^2 kg^{-1}) of $GdAl_2/Al_2O_3$ nanocapsules,[8] although some Dy_2O_3 nanoparticles exist in the sample, which decrease the mass that is effective in the magnetic measurement (due to their mixture with $DyCo_2$) of the powder mixture. The reason is that $DyCo_2$ has a larger magnetic moment of $7.83\mu_B$, than $GdAl_2$ $(7.2\mu_B)$ and as a result the $DyCo_2$ system has a moment density higher than that of $GdAl_2$ system.[8,10]

Avoiding the difference between ZFC and field-cooled (FC) processes, which is typical for superparamagnetic particles in low fields, the ΔS_M of the magnetic nanoparticles can be defined between two states at finite magnetic-field values.[8] The ΔS_M of the nanoparticles can be derived by using the Maxwell relationship given by $\Delta S_M(T,B)=\int_{B1}^{B2}(\partial M/\partial T)_B dB$. In Fig. 3(b), by using the numerical approximation $\Delta S[(T_{n+1}+T_n)/2,B]=\Sigma[(M_{n+1}-M_n)/(T_{n+1}-T_n)]\Delta B$,[11] the calculated $-\Delta S_M$ values of $DyCo_2$ nanoparticles are shown as a function of temperature (varying between 5 and 90 K) after a field change of 6 T. It is interesting to note that $-\Delta S_M$ rapidly increases with decreasing temperature and reaches the largest value of 13.2 J kg^{-1} K^{-1} at 7.5 K. For conventional MCE materials, the large $-\Delta S_M$ generally appears near the transition temperature of the first-order magnetostructural or the second-order magnetic transition. According to the ZFC-FC magnetization curves shown in Fig. 3(c), however, no phase transition occurs in the present sample at temperatures between 5 and 90 K at 1 T. The rapid increase in dM/dT value with decreasing temperature [see the inset of Fig. 3(c)] indicates that the $DyCo_2$ nanoparticles have a large $(\partial M/\partial T)_B$,

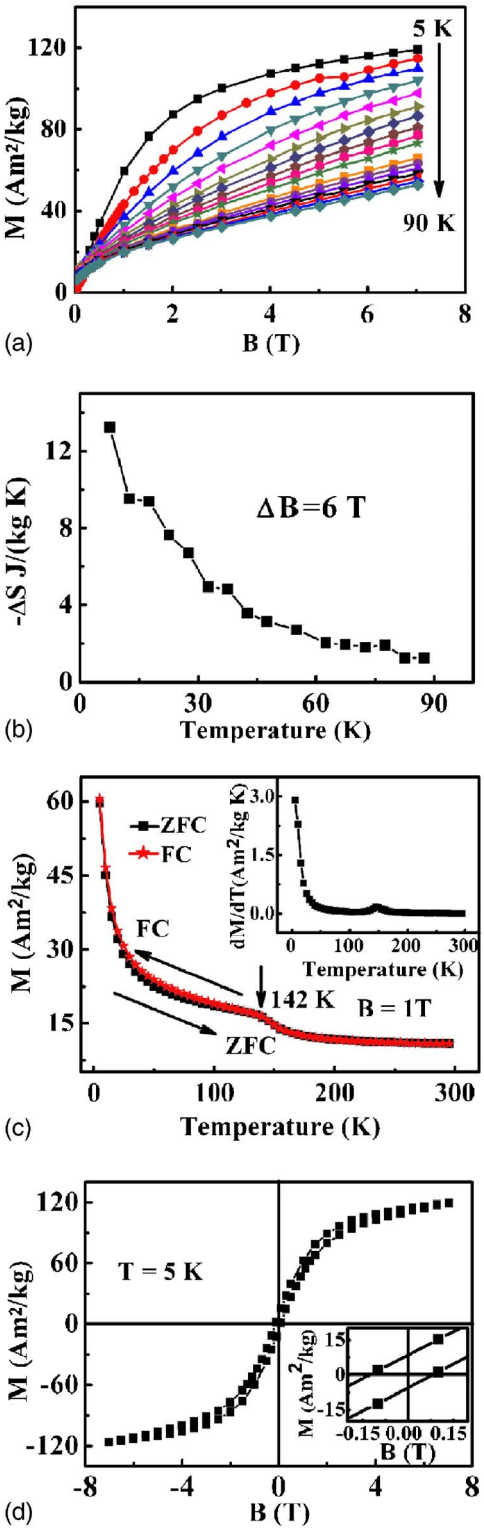

FIG. 3. (Color online) (a) Isothermal magnetization curves obtained at different temperatures in ZFC process. (b) Temperature dependence of the magnetic-entropy change between 5 and 90 K in a field variation from 1 to 7 T. (c) ZFC and FC magnetization curves between 5 and 300 K, obtained in an applied field of 1 T. (d) Hysteresis loop of $DyCo_2$ nanoparticles obtained at 5 K. The inset shows an enlarged part of magnetization curve.

generating a large $-\Delta S_M$ in the low-temperature range, according to the Maxwell relationship.

It has been reported that $DyCo_2$ nanoparticles show superparamagnetic behavior below their Curie temperature of 142 K (little lower than 145 K of bulk $DyCo_2$).[10] The magnetic nanoparticles, however, may enter the spin-glass state due to the strong interaction between them, if they are pressed together for the magnetic measurement. In the present case, according to Fig. 3(c), such strong interaction can be excluded due to (i) the overlap of the ZFC-FC curves in the applied field of 1 T, indicating reversible behavior in the ZFC and FC processes,[12] and (ii) the value of the paramagnetic Curie temperature $\theta=-4.5$ K by extrapolation of the reciprocal dc susceptibility of the FC curve, which is quite different from the corresponding value $\theta=-170$ K of the spin-glass system.[12,13] The reason for the weak interaction among the $DyCo_2$ nanoparticles is the presence of nonmagnetic Dy_2O_3 particles that mixed with $DyCo_2$ particles and prevent adequate physical contact of the $DyCo_2$. Furthermore, the magnetization variation of superparamagnetic $DyCo_2$ nanoparticles is determined by the Zeeman energy, thermal-excitation energy (k_BT), anisotropy-energy barrier, and weak interaction energy, which have both excitation and hindrance effect on the rotation of the magnetic moments. At a certain low temperature and a constant magnetic field (for instance at 5 K and 7 T), these four kinds of energies maintain a balance. When the temperature and applied field are changed, the balance among these energies will be disturbed and, as a result, the Zeeman energy and k_BT will help to overcome the hindrance of the anisotropy-energy barrier and the weak interaction energy to change the orientations of the magnetic moments. Due to the presence of a high moment density in the $DyCo_2$ nanoparticles, the variation of temperature and magnetic field will force a large amount of moments to change their orientation. A large change of magnetic order will therefore be generated, leading to large $(\partial M/\partial T)_B$. On the other hand, the coercivity depends strongly on the anisotropy-energy barriers. The coercive force of 0.0854 T of the $DyCo_2$ nanoparticles is much higher than that of $GdAl_2/Al_2O_3$ nanocapsules (0.0291 T) at 5 K, which indicates the higher anisotropy-energy barrier of the former [Fig. 3(d)].[14] Although the appearance of large anisotropy-energy barriers reinforces the hindrance of the rotation of the $DyCo_2$ moments, the large moment density still assures the large $-\Delta S_M$ of 13.2 J kg^{-1} K^{-1} at 7.5 K with $\Delta B=6$ T. Moreover, the existence of nonmagnetic Dy_2O_3 nanoparticles also leads to the deterioration of $-\Delta S_M$ because, when mixed with $DyCo_2$ nanoparticles, they decrease the effective mass of the samples.

In conclusion, nanoparticles without encapsulation of the intermetallic compound $DyCo_2$ have been prepared by a modified arc-discharge technique. The irregular spherical-shaped $DyCo_2$ nanoparticles are of good crystallinity, which are stable and exist in air without protection of any shells. In a field change ΔB of 6 T, $-\Delta S_M$ of the $DyCo_2$ nanoparticles quickly increases with decreasing temperature from 90 to 5 K and reaches a maximum of 13.2 J kg^{-1} K^{-1} at 7.5 K. The large $-\Delta S_M$ of the $DyCo_2$ nanoparticles is a result of the large magnetic moment density and the weak interaction energy. These $DyCo_2$ nanoparticles may be as very promising magnetocaloric material for low-temperature refrigeration applications.

This work was supported by National Natural Science Foundation of China under Grant No. 50331030.

[1] V. K. Pecharsky and K. A. Gschneidner, Jr., Phys. Rev. Lett. **78**, 4494 (1997).
[2] F. X. Hu, B. G. Shen, J. R. Sun, Z. H. Cheng, G. H. Rao, and X. X. Zhang, Appl. Phys. Lett. **78**, 3675 (2001).
[3] H. Wada and Y. Tanabe, Appl. Phys. Lett. **79**, 3302 (2001).
[4] O. Tegus, E. Brück, K. H. J. Buschow, and F. R. de Boer, Nature (London) **415**, 150 (2002).
[5] T. A. Yamamoto, M. Tanaka, T. Nakayama, and K. Niihara, Jpn. J. Appl. Phys., Part 1 **39**, 4761 (2000).
[6] X. X. Zhang, H. L. Wei, Z. Q. Zhang, and L. Zhang, Phys. Rev. Lett. **87**, 157203 (2001).
[7] M. Evangelisti, A. Candini, A. Ghirri, and E. J. K. Mclnnes, Appl. Phys. Lett. **87**, 072504 (2005).
[8] S. Ma, W. F. Li, D. Li, D. K. Xiong, N. K. Sun, D. Y. Geng, W. Liu, and Z. D. Zhang, Phys. Rev. B **76**, 144404 (2007).
[9] Z. D. Zhang, J. Mater. Sci. Technol. **23**, 1 (2007).
[10] A. Kowalczyk, J. Baszyński, A. Szajek, J. Kováč, and I. Škorvánek, J. Magn. Magn. Mater. **152**, L279 (1996).
[11] L. H. Lewis, M. H. Yu, and R. J. Gambino, Appl. Phys. Lett. **83**, 515 (2003).
[12] M. Garcia del Mruo, X. Battle, and A. Labarta, J. Magn. Magn. Mater. **221**, 26 (2000).
[13] Y. Sun, M. B. Salamon, K. Garnier, and R. S. Averback, Phys. Rev. Lett. **91**, 167206 (2003).
[14] C. de Julian Fernandez, Phys. Rev. B **72**, 054438 (2005).